

A New Daily Observational Record from Grytviken, South Georgia: Exploring Twentieth-Century Extremes in the South Atlantic

ZOË THOMAS,^{a,b} CHRIS TURNEY,^{a,b} ROB ALLAN,^c STEVE COLWELL,^d GAIL KELLY,^c
DAVID LISTER,^e PHILIP JONES,^{e,f} MARK BESWICK,^g LISA ALEXANDER,^{b,h}
TANYA LIPPMANN,ⁱ NICHOLAS HEROLD,^{b,h} AND RICHARD JONES^j

^a *Palaeontology, Geobiology and Earth Archives Research Centre, School of Biological,
Earth and Environmental Sciences, University of New South Wales, Sydney,
New South Wales, Australia*

^b *Climate Change Research Centre, School of Biological, Earth And Environmental Sciences,
University of New South Wales, Sydney, New South Wales, Australia*

^c *Met Office Hadley Centre/ACRE, Exeter, United Kingdom*

^d *British Antarctic Survey, Cambridge, United Kingdom*

^e *Climatic Research Unit, School of Environmental Sciences,
University of East Anglia, Norwich, United Kingdom*

^f *Center of Excellence for Climate Change Research,*

Department of Meteorology, King Abdulaziz University, Jeddah, Saudi Arabia

^g *National Meteorological Library and Archive, Met Office, Exeter, United Kingdom*

^h *ARC Centre of Excellence for Climate System Science,*

University of New South Wales, Sydney, New South Wales, Australia

ⁱ *Faculty of Earth and Life Sciences, Vrije Universiteit Amsterdam, Amsterdam, Netherlands*

^j *Department of Geography, Exeter University, Devon, United Kingdom*

(Manuscript received 28 May 2017, in final form 12 November 2017)

ABSTRACT

The sparse nature of observational records across the mid- to high latitudes of the Southern Hemisphere limits the ability to place late-twentieth-century environmental changes in the context of long-term (multi-decadal and centennial) variability. Historical records from subantarctic islands offer considerable potential for developing highly resolved records of change. In 1905, a whaling and meteorological station was established at Grytviken on subantarctic South Georgia in the South Atlantic (54°S, 36°W), providing near-continuous daily observations through to present day. This paper reports a new, daily observational record of temperature and precipitation from Grytviken, which is compared to regional datasets and historical reanalysis. The authors find a shift toward increasingly warmer daytime extremes commencing from the mid-twentieth century and accompanied by warmer nighttime temperatures, with an average rate of temperature rise of 0.13°C decade⁻¹ over the period 1907–2016 ($p < 0.0001$). Analysis of these data and reanalysis products suggest a change of pervasive synoptic conditions across the mid- to high latitudes since the mid-twentieth century, characterized by stronger westerly airflow and associated warm föhn winds across South Georgia. This rapid rate of warming and associated declining habitat suitability has important negative implications for biodiversity, including the survival of key marine biota in the region.

1. Introduction

Climate changes in the mid- to high latitudes of the Southern Hemisphere have exhibited extreme and regionally asymmetric trends in temperature and precipitation over the last half century, with warming particularly marked over the Antarctic Peninsula and the South Atlantic (Turner et al. 2005; Abram et al.

2014; Richard et al. 2013; Turney et al. 2016c; J. Jones et al. 2016). However, because of the sparse distribution and temporal limitations of instrumental records, the long-term evolution of climatically sensitive high-latitude regions of the Southern Hemisphere, especially prior to the 1950s, remains elusive. Subantarctic islands are particularly important in this regard, straddling major ocean and atmospheric boundaries, and offer the potential to develop highly resolved records of near open-ocean conditions. The

Corresponding author: Zoë Thomas, z.thomas@unsw.edu.au

DOI: 10.1175/JCLI-D-17-0353.1

© 2018 American Meteorological Society. For information regarding reuse of this content and general copyright information, consult the AMS Copyright Policy (www.ametsoc.org/PUBSReuseLicenses).

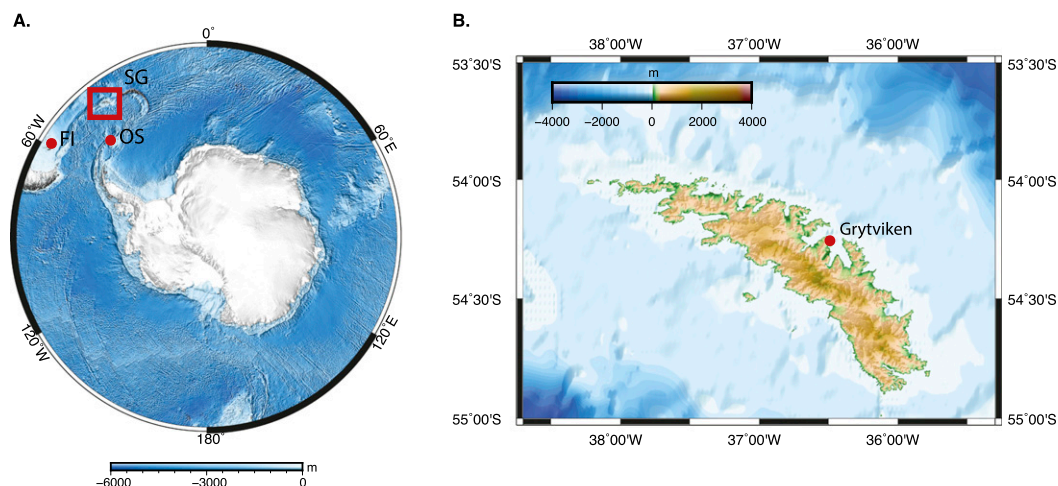


FIG. 1. Location of (a) South Georgia (SG; red square), the Falkland Islands (FI) and Orcadas Station (OS) (both red dots), and (b) the meteorological station at Grytviken in Cumberland Bay (red dot).

ecosystems that inhabit these islands are of global importance, with high biological diversity and productivity, but appear to be increasingly vulnerable to late-twentieth-century change (Boyd et al. 2015; Constable et al. 2014; Trathan et al. 2012; Turney et al. 2017). Proxy reconstructions have shown that the circumpolar Antarctic has experienced major changes in the patterns and strengths of dominant airflow over recent millennia (J. Jones et al. 2016; Turney et al. 2016a; Anderson et al. 2009), with associated implications for carbon uptake (Le Quéré et al. 2009; Turney et al. 2016b; Sallée et al. 2012; Landschützer et al. 2015). To provide a baseline for contemporary and future changes, high-resolution (subannual to annual) observational records are urgently required across the region. Although invariably remote, numerous whaling stations were established across the Southern Ocean islands in the late nineteenth and early twentieth centuries, where in some locations, daily weather observations were meticulously recorded.

South Georgia is a relatively small, mountainous, and heavily glaciated subantarctic island ($\sim 3500 \text{ km}^2$) located in a strategic location for understanding Southern Ocean atmosphere–ocean dynamics, approximately 1500 km northeast of the Antarctic Peninsula (Fig. 1). It has experienced substantial glacier retreat during the second half of the twentieth century, with particularly dramatic losses during the first decade of the twenty-first century (Cook et al. 2010; Gordon et al. 2008). While the precise drivers of this glacier retreat remain unclear, the large impacts of this retreat on the terrestrial and marine biota makes an understanding of these drivers all the more crucial (Cook et al. 2010; Murphy et al. 2007). Despite the value of historical

data for expanding the observational network, only a monthly resolved dataset has until now been available.

Crucially, South Georgia was home to numerous whaling stations from 1905, one of which, the station at Grytviken, provides the longest and most complete meteorological records on the island. Although monthly climate statistics from subantarctic South Georgia are currently available in the public domain (<https://legacy.bas.ac.uk/met/READER>), understanding changes in temperature and precipitation extremes requires daily resolved data. A coordinated effort was therefore undertaken to locate and transcribe the records from Grytviken to improve our understanding of South Atlantic climate change through the twentieth century. Importantly, this contribution will add to the Atmospheric Circulation Reconstructions over the Earth (ACRE)-facilitated reanalyses database, providing crucial data in a data-sparse region and time period. In this paper, we explore this unique daily record of changes in the averages and extremes of climate over the twentieth century.

2. Data and methods

The establishment of a whaling and meteorological station at Grytviken, South Georgia [also known as Cumberland Bay or King Edward Point, located on the north coast of South Georgia (World Meteorological Organization station 88903; $54^{\circ}16'59''\text{S}$, $36^{\circ}30'0''\text{W}$)], in 1905 resulted in the creation of one of the longest observational records from the high latitudes of the Southern Hemisphere. Between 1905 and 1950, the occupying Norwegian–Argentine whaling station

(Compania Argentina de Pesca) took meteorological readings. Following this, the British Falkland Island Dependencies Survey (and later, British Antarctic Survey) took ownership of the station until the outbreak of the South Atlantic Conflict in April 1982. A small British military garrison reoccupied the station weeks later, where they remained until March 2001. Near-continuous measurements were taken from 1905 to 1982, and although it is believed that the military did take meteorological readings, uncertainty over the station layout and the ultimate location of the observational registers has unfortunately resulted in an 18-yr gap in the record. Monthly data from 1984–88 are available from the British Antarctic Survey, but so far, no daily data or metadata have been identified. We therefore exclude these data (1984–88) from our analyses and highlight the unverified data where shown. Upon the departure of the military, the British Antarctic Survey installed an automatic weather station (AWS) in March 2001, providing continuous measurements through to the present day.

The Grytviken weather station is located at an altitude of 2.2 m above mean sea level. The data from the early Norwegian–Argentine occupation from 1905 to 1962 are archived at the National Meteorological Library and Archive in Exeter, United Kingdom, and from 1963–82 at the British Antarctic Survey Archives in Cambridge, United Kingdom. Data from the automated weather station, operating since 2001, can be accessed online (https://legacy.bas.ac.uk/cgi-bin/metdb-form-2.pl?tableouse=U_MET.GRYTVIKEN_AWS&complex=1&idmask=.....&acct=u_met&pass=weather). The data elements transcribed in this study were daily maximum temperatures (TX), daily minimum temperatures (TN), and daily precipitation totals (PREC).

Metadata for the meteorological station at Grytviken are available, including height above ground, particulars of the instruments, and dates and details of any station/instrument location changes. Importantly, these metadata allow us to evaluate and cross-check our homogeneity tests to confirm the integrity of the record. For instance, when the station changed hands from Argentine to British control, metadata from the station read: “The former station closed in 1948 and was replaced by King Edward Point, the two sites should be compatible. Reliability: compared with 88890 [Stanley] and 87968 [Orcadas] for the years 1923–1980 and 1905–1980.” It was established from the metadata that temperature data from January 1905 to June 1907 should be discounted because of faulty exposure of the thermometers, which were affected by solar radiation, providing erroneously high readings. Although the thermometer screen was reported to have moved in January 1978, there is no evidence that this created a difference in the

temperature readings. However, there are no known metadata available when the station was under military control, apart from unconfirmed reports that the thermometer screen was moved next to a building. The Milos 500 AWS was installed in March 2001, providing hourly readings, and was replaced by a Milos 530 AWS in 2006, which records 1-min observations. Both AWSs used a platinum resistance thermometer probe with an accuracy of $\pm 0.2^{\circ}\text{C}$. In terms of precipitation data, up to 1982 measurements were taken with a Snowdon rain gauge, which can underread in snow conditions, as the wind can blow some of the snow over the top of the gauge (Goodison et al. 1998). The data since 2010 have been collected using a laser precipitation monitor, which is thought to be more accurate. However, as there is no overlap between the two instrumentation methods, there is no way to assess how different the totals are; thus, long-term trends that include data using both instruments should be interpreted with extreme caution. Homogeneity tests were undertaken to detect and adjust for sudden step changes present in the time series for reasons other than climatic changes (such as instrument change) using the software package RHTestsv4 (Wang 2008a,b; Wang and Feng 2013), but we found no significant inhomogeneities in the daily precipitation, maximum, or minimum temperature data.

Basic quality controls have been undertaken for all series following the procedures outlined in Alexander et al. (2006) and, where necessary, unreliable data removed. Missing data criteria were adapted from Zhang et al. (2011) and applied as follows: monthly indices were calculated if no more than 3 days were missing in a month, seasonal indices were calculated if no more than 6 days were missing in the 3-month period (and no more than 4 days missing per month), and annual values were calculated if no more than 15 days were missing in a year and no single month was missing. In addition to the missing data between March 1982 and March 2001, there were several other gaps in the observations associated with observer illness or instrumentation problems affecting the following periods: October 1910–May 1911; January 1919–April 1920; March–April 1928; and May 1946–December 1949. After the AWS was installed in 2001, there were occasional issues with the automatic instrumentation and/or computer that could take several days to resolve (this was particularly acute during 2007). In addition, the data were removed between September 1968 and December 1969, owing to suspect diurnal temperature range and unusually high precipitation values. It is worth noting that while rarely transcribed, observational registers often have valuable qualitative data in addition to the quantitative data recorded. Following identification of potentially spurious

value(s), we examined the original observational registers to help identify any transcription errors as well as any qualitative comments made that could help to corroborate the values. For example, in August 1939, the mean monthly temperature appeared anomalously low. The register was consulted, and it was determined that there were no transcription errors. Instead, comments in the “observations” section had several phrases indicating particularly cold conditions: “muy frio” (very cold), “ventisca dia y noche” (blizzard day and night), “viento fuerte” (strong wind), and “temperatura muy baja” (temperature very low). Qualitative data such as these can be valuable sources of extra quality assurance.

The data were analyzed with the R-based CLIMACT software package (Alexander and Herold 2015) to calculate selected extreme climate indices (Zhang et al. 2011). We used daily minimum (TN) and maximum (TX) temperature as well as daily precipitation in this assessment. Percentile-based threshold levels, including the 10th and 90th percentiles of the daily minimum (TN10p) and maximum (TX90p) temperatures (with 1950–80 as our baseline), were used to measure changes in moderate extremes. To calculate rates of change, we used a generalized least squares approach, fit by maximizing the restricted log-likelihood (REML) with autoregressive (AR) errors, to estimate the slope term of an assumed linear trend. We utilized the Akaike information criterion (AIC) to compare different models and chose an autoregressive model of order AR(1), which successfully removed autocorrelation of the residuals. The trends are reported as degrees Celsius of warming per decade or precipitation sum (mm) increase per decade calculated for each period, with the associated standard error and p value provided. Unfortunately the 20-yr gap in the record precludes analysis identifying whether the changes over time are the result of an underlying system threshold (Thomas 2016) or linear response to forcing. Instead, to further explore the atmospheric drivers of observed climate changes, we also used the ACRE-facilitated NOAA-CIRES Twentieth Century Reanalysis project version 2c (20CRv2c) (Compo et al. 2011; Giese et al. 2016). The data from this study will be publically accessible via the ISTI (International Surface Temperature Initiative; <http://www.surface temperatures.org/>) and the GPCC (Global Precipitation Climatology Centre; <https://www.esrl.noaa.gov/psd/data/gridded/data.gpcc.html>).

3. Results

A warming trend over the twentieth century at Grytøyen is observed in mean monthly temperature derived from daily data (calculated as the average of TX and TN)

(Fig. 2a), with an average annual temperature rise of $0.13^{\circ}\text{C decade}^{-1}$ over the period 1907–2016 ($p < 0.0001$; Table 1). However, more detailed analysis of this rate of increase shows a slight decrease in temperatures over the first two decades of the record at South Georgia, before the warming trend was established. When splitting the record approximately in half (1906–50 and 1951–2016), there is no significant trend identified in the early half of the twentieth century, but there is a strong trend in the latter half, peaking at $0.22^{\circ}\text{C decade}^{-1}$ in summer ($p < 0.001$; Table 1). Importantly, however, the rate of warming is not constant year round. When seasonal trends are investigated, the largest warming trend occurs during the austral spring and summer months (Table 1).

To determine whether the AWS station was reporting temperatures that would bias the trends, we compared the decadal rates of change calculated over 1951–2017 with those for the period excluding the AWS data (1951–83) and found them to be generally consistent (though with a lower p value, accordant with a smaller number of observations; Table 1). We also compared the observations from South Georgia to the ACRE-facilitated 20CRv2c (Fig. 2b). This comparison showed a weak but statistically significant correspondence between the two time series (Pearson product-moment correlation of 0.347, $p < 0.0043$), though it is important to note that due to South Georgia’s small size, the reanalysis assigns the location as an ocean cell rather than a land cell, which most probably explains the lower variability in the reanalysis time series (in the future, this resolution will be improved in 20CRv3 through downscaling of its output). We also calculated the decadal rates of change over the same time periods for the reanalysis data as for the observations, reported in Table 1. These show coherence to the observational trends in all periods, suggesting that the data from the AWS have not biased the linear trend since 1950.

To investigate the distribution of temperatures across the seasons more fully, we explored the probability distribution functions for daily seasonal temperatures at South Georgia over each 20-yr period since 1907 (Fig. 3). Although the shape of the distributions remains largely unchanged (with only a slight shift to a more positively skewed distribution between the first and second half of the twentieth century in all seasons), TX and TN appear to have shifted toward warmer values through the twentieth century. Most notably, the overall distribution in TX and TN appears to have remained largely unchanged across the period 1907–66, but subsequent bidecadal averages show a uniform shift to higher temperatures, most notably during the austral spring and summer. This shift implies that there was a change in the frequency of occurrence of cold and warm extremes across the mid-twentieth century, with more

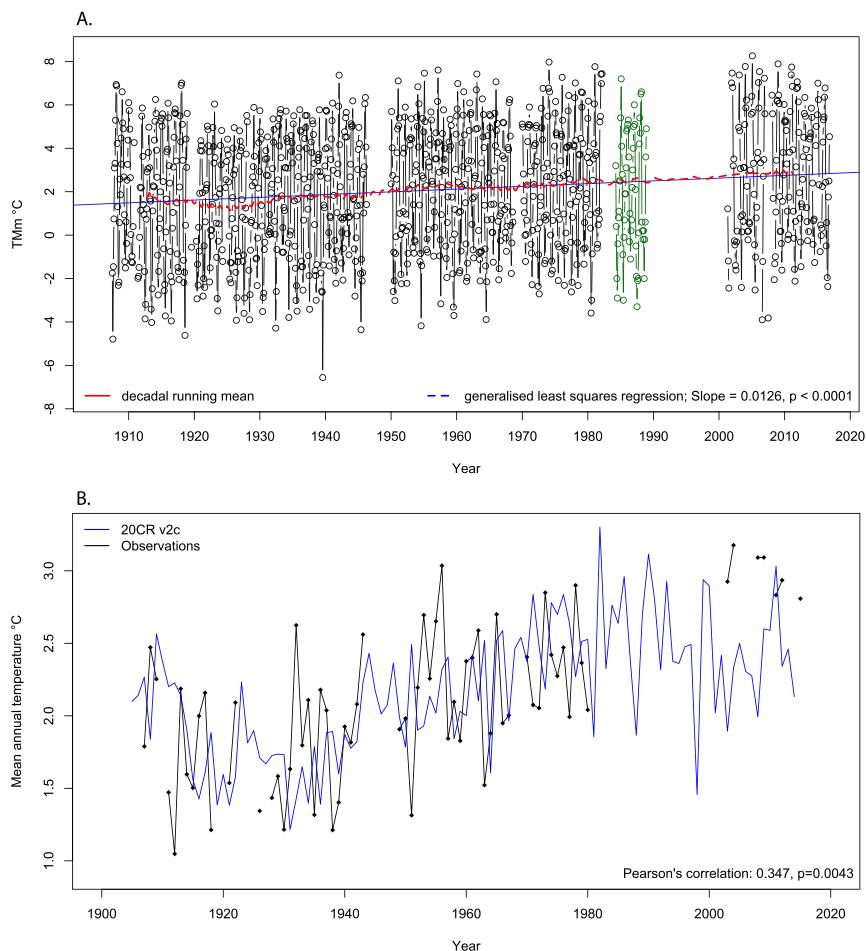


FIG. 2. (a) Average mean monthly temperature from South Georgia, with generalized least squares regression (blue) and decadal running mean (red) lines shown. Dark green data (1984–88) from the military station are unverified and not included in the linear regression or decadal running mean. (b) Annual (July–June) 1000-hPa air temperature from 20CRv2c (blue), plotted against South Georgia mean annual (July–June) temperature from observations (black).

frequent warm extremes and less frequent cold extremes experienced over recent decades, compared to the beginning of the twentieth century.

Because some weather extremes are predicted to become more frequent due to anthropogenic forcing (IPCC 2012), extremes over the past century can provide a baseline to compare modern variability, a situation exacerbated in the mid- to high latitudes of the South Atlantic where the observational record is particularly limited. Since extremes are inherently rare events, we look at “moderate” extreme indices, defined as those that occur several times per year, rather than rarer events, whose statistics would be harder to robustly characterize (Sardeshmukh et al. 2015; Zhang et al. 2011). To further explore the changes of warm and cool extremes during the summer and winter, we therefore analyzed the change in the frequency of occurrence of temperatures exceeding the 10th and 90th percentiles

(TN10p and TX90p), using the period 1950–80 as a baseline. Here we observe an increase in the frequency of moderate warm extremes during the austral summer [December–February (DJF)] and a decrease in the occurrence of moderate cool extremes during winter [June–August (JJA)] (Fig. 4). The mean minimum temperature in DJF increased from 1.05°C in 1907–26 to 1.61°C in 1947–66 and to 2.47°C in 2001–16, with their standard deviations at 2.14°, 1.96°, and 2.30°C, respectively. A similar pattern was found for the mean maximum temperature in DJF, which increased by a total of 1.5°C over the same period.

Analysis of the annual precipitation total (using only totals with <6 missing observations per year) shows a strong increasing trend through the twentieth century (Fig. 5), representing an average increase of $\sim 40 \text{ mm yr}^{-1}$ (though this is superimposed on a highly variable time series). A marked shift in the amount of precipitation is

TABLE 1. Trends ($^{\circ}\text{C decade}^{-1}$) for mean monthly mean temperature and seasons, with standard error and p values for selected periods of time (** where $p < 0.01$; * where $p < 0.05$; * where $p < 0.1$) for South Georgia observations and 20CRv2c.

	1907–50	1950–2016	1951–83	1907–2016
South Georgia observations				
TM annual	−0.097	0.11***	0.14	0.13***
Std. err.	0.0107	0.0037	0.0090	0.0026
p value	0.370	0.0043	0.143	8.36×10^{-6}
TM SON	−0.14	0.14**	0.19	0.14***
Std. err.	0.0134	0.005	0.015	0.0034
p value	0.291	0.012	0.221	9.32×10^{-5}
TM DJF	−0.01	0.22***	0.31**	0.16***
Std. err.	0.014	0.006	0.014	0.003
p value	0.970	0.001	0.030	1.14×10^{-5}
TM MAM	−0.09	0.03	−0.07	0.08**
Std. err.	0.0133	0.0063	0.0165	0.0032
p value	0.506	0.703	0.684	0.0159
TM JJA	0.13	0.09*	0.06	0.16***
Std. err.	0.014	0.005	0.014	0.003
p value	0.370	0.068	0.660	1.85×10^{-6}
20CRv2c				
TM annual	0.01***	0.04**	0.21***	0.08***
Std. err.	0.952	0.123	0.0001	0.0017
p value	0.009	0.003	0.004	1.31×10^{-5}

observed from the most recent period (2010–16), but due to possible inhomogeneities caused by instrument changes from 2010 (though none were detected in our tests, there is a 28-yr gap between the two types of instrument), it remains unclear how significant this is. It is possible that the increasing precipitation trend described above may have resulted in more precipitation falling as rain, rather than snow, which is better recorded (Førland and Hanssen-Bauer 2000; Hanssen-Bauer 2002; Førland and Hanssen-Bauer 2001). It is noted, however, that even omitting the 2010–16 precipitation values still results in a significant increasing trend in annual precipitation totals (Fig. 5, Table 2). To understand the seasonal variation in rainfall, we divided the data into seasons: DJF, March–May (MAM), JJA, and September–November (SON), where there is a clear bias toward higher precipitation in autumn and winter (Fig. 6). In addition, the trajectory of the locally weighted scatterplot smoothing lines indicates a greater rate of increase in precipitation in these seasons (and with lower totals, but similar rates of increase in SON), suggesting that whatever mechanism is driving the increase in precipitation, it dominates in autumn and winter.

4. Discussion

The warming trends observed at Grytviken, South Georgia, are comparable to the trends from the nearby

Orcadas station on Laurie Island, on the eastern side of the Antarctic Peninsula (Zazulie et al. 2010). The total amount of annual mean warming at Grytviken between 1907 and 2016 is 1.42°C ($p < 0.0001$; Table 1), equivalent to an average rate of $0.13^{\circ}\text{C decade}^{-1}$, similar to the $0.2^{\circ}\text{C decade}^{-1}$ observed at Laurie Island (1903–2008) (Zazulie et al. 2010). A strong seasonal component is identified in the South Georgia dataset, however, with the austral summer months contributing most to the annual trend, particularly during the second half of the twentieth century (1951–2017; $0.22^{\circ}\text{C decade}^{-1}$, $p < 0.001$; Table 1). Similar seasonal differences in trends are also observed at Orcadas, with the rate of summer warming in the latter half of the twenty-first century double that of the early twenty-first century (Zazulie et al. 2010). In contrast, the linear trend of the temperature series from the Falkland Islands between 1920 and 2010 is $0.05^{\circ}\text{C decade}^{-1}$ ($p = 0.002$) (Lister and Jones 2014; P. Jones et al. 2016), which is substantially lower than South Georgia.

It is important to note that many warm extremes on South Georgia relate to föhn winds, which are defined as strong, warm, dry winds that descend from mountains (Skansi et al. 2017). South Georgia's climate is strongly modified by the steep orography, with a high mountain chain $>2000\text{ m}$ above mean sea level running down the spine of the island. Located within the belt of the westerly winds, the island acts as a natural barrier to the prevailing airflow. Strong prevailing airflow over a topographic obstacle results in an adiabatic cooling of the rising air at the moist-adiabatic lapse rate, causing latent heat to be released and precipitation to occur, while decreasing the humidity of the advected air. As the parcel then starts to descend down the leeward slope, it warms at the faster dry-adiabatic lapse rate, resulting in a temperature and humidity gradient between the windward and leeward sides of the topographic barrier at the same elevation (Elvidge and Renfrew 2016; Skansi et al. 2017). Föhn warming can also take place without precipitation, where warming on the leeside of a topographic barrier can be generated by the descent of warmer air sources above it caused by blocked flow (Elvidge and Renfrew 2016). These föhn winds have been shown to be frequent, occurring approximately every 4 days, and capable of increasing the temperature by up to 20°C , with a mean increase in temperature across all events of $\sim 10^{\circ}\text{C}$ (as measured between 2003 and 2013) (Bannister and King 2015). While wind speed and direction have been recorded at South Georgia since 1905, these variables have not yet been transcribed (in part due to the notorious unreliability of historical observational wind data over highly variable terrain), limiting our understanding of the role föhn winds have played during the twentieth century. However, wind

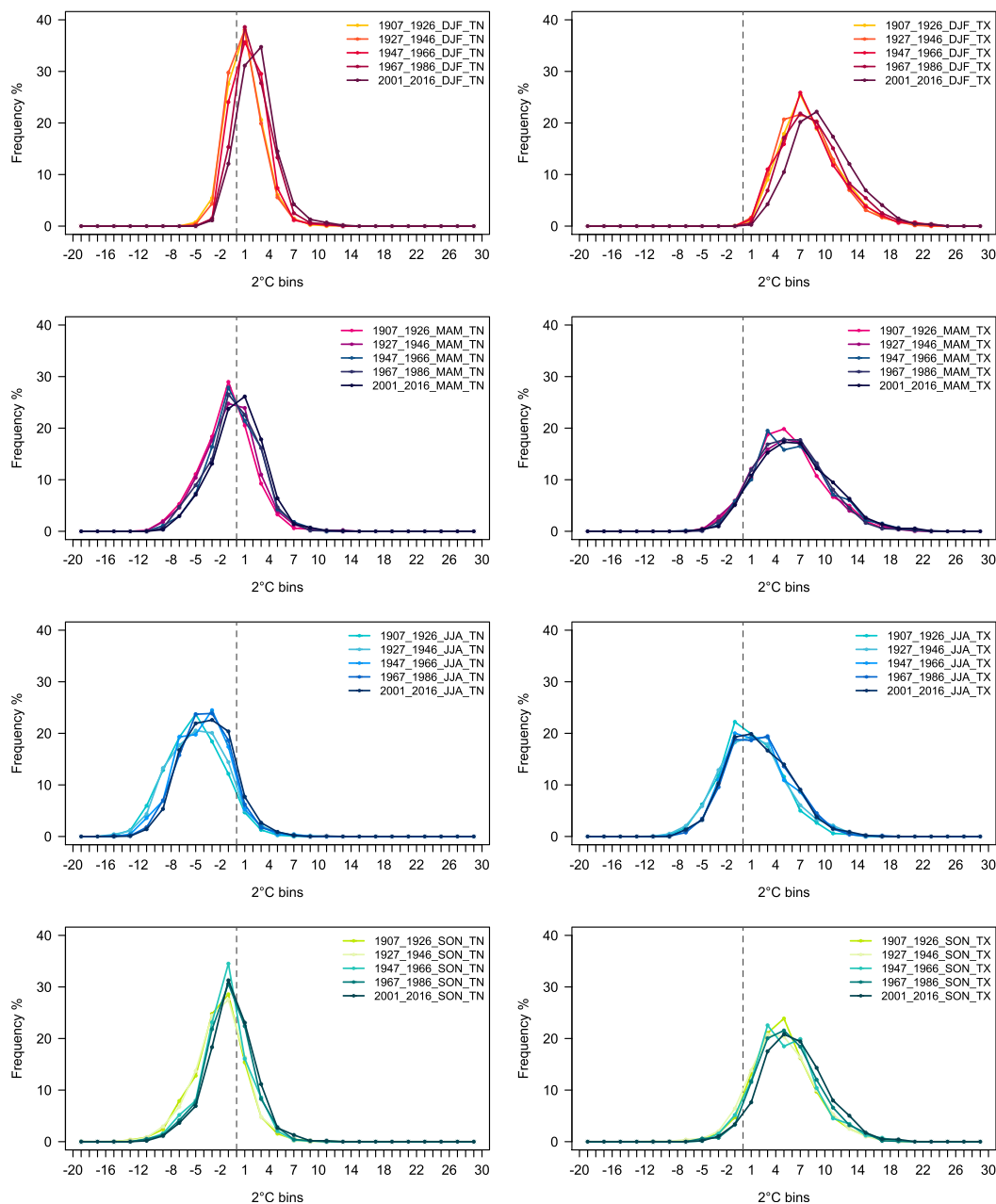


FIG. 3. Distribution of frequencies of daily (left) minimum (TN) and (right) maximum (TX) temperatures during DJF, MAM, JJA, and SON for 20-yr periods since 1907. Note the data gap between 1983 and 2001. The dashed line is at 0°C, and 2°C bins have been used.

speed and direction have been measured with the AWS on South Georgia since installation in 2001, though unfortunately, because of local topographic modification (e.g., wind channeling), the recorded wind direction at King Edward Point is not indicative of the synoptic wind pattern. Instead, in [Bannister and King \(2015\)](#), ERA-Interim was used to illustrate synoptic conditions during föhn events and showed a well-defined ridge of high pressure, centered just north of

South Georgia during strong föhn conditions, a feature that is absent in the climatological mean.

There are several important modes of variability that affect climate and weather in the high latitudes of the South Atlantic. For instance, the Pacific–South American (PSA) teleconnection pattern is one through which the El Niño–Southern Oscillation (ENSO) signal propagates into high southern latitudes during the austral spring/summer ([Mo and Higgins 1998](#); [Ding et al. 2012](#)),

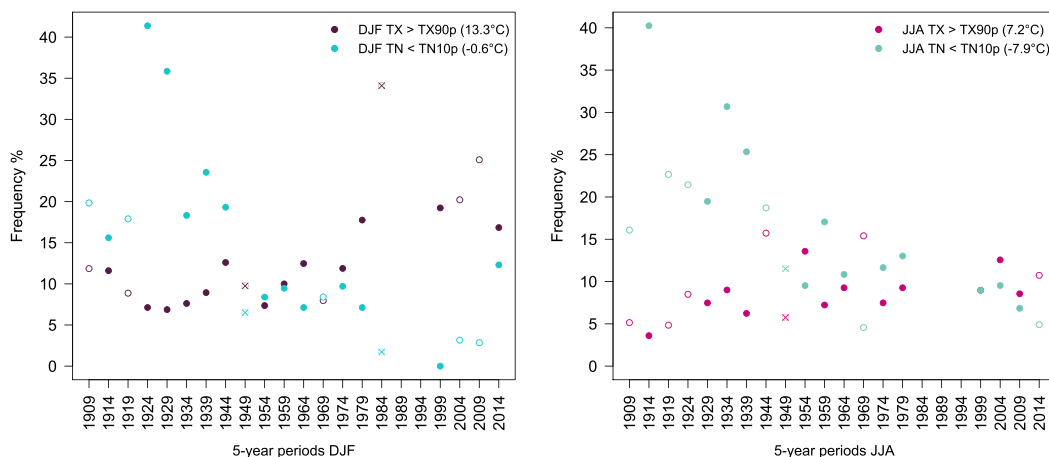


FIG. 4. Changes in the percentages (left) of relatively warm days (TX90p; purple) and cold days (TN10p; blue) for 5-yr periods for DJF, and (right) of relatively warm days (TX90p; pink) and cold days (TN10p; green) for 5-yr periods for JJA. Open circles indicate periods where only 3 or 4 years of data were available; crosses indicate where 1 or 2 years of data were available.

causing strong northerlies to advect warm maritime air from the South Pacific toward South Georgia. An increase in Rossby wave penetration, thought to be linked to tropical Pacific temperatures, has been suggested to play a potential role in the evolution of Antarctic climate since the mid-twentieth century (Fogt et al. 2011; Ding et al. 2012; Turney et al. 2017, 2016c).

The major mode of variability in atmospheric circulation in the high southern latitudes, however, is the southern annular mode (SAM): a circumpolar circulation pattern defined by the zonal mean atmospheric pressure difference between 40° and 65°S (Marshall 2003; Thompson et al. 2011). The multidecadal trend to a more positive SAM since the mid-twentieth century (Abram et al. 2014) is manifested by a strengthening and southward shift of westerly airflow over the Southern

Ocean (Visbeck 2009; Marshall 2003; Thompson et al. 2011). Although an increase in the SAM index has occurred in all seasons, the most pronounced trend is observed over the summer and autumn (Marshall 2003). The impact of SAM may have been amplified as a result of the spring Antarctic ozone hole, established in the late 1970s, and exerts its greatest effect on climate and circulation patterns during the summer (Thompson and Solomon 2002; Zazulie et al. 2010). However, the warming trend observed from South Georgia starts before this time, suggesting that ozone cannot be the sole driver of the warming trends observed. Indeed, although of a smaller magnitude, warming is also observed in the winter months.

The precipitation trends observed from South Georgia differ in two main aspects to the temperature trends:

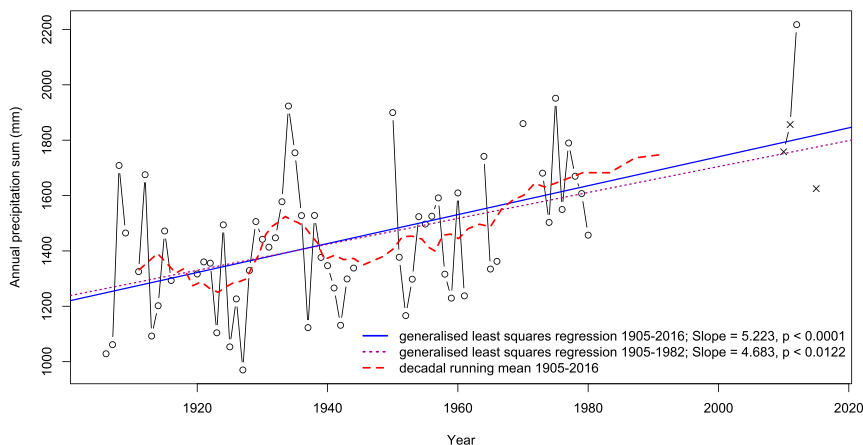


FIG. 5. Annual (July–June) precipitation totals (mm), including only years with no missing observations (open circles), and years with <6 missing days per year (crosses), with linear regressions for the years 1905–82 and 1905–2016 and a decadal running mean (1905–2016).

TABLE 2. Trends [precipitation sum (mm) per decade] for mean monthly precipitation sum, with standard error and p values for selected periods of time (** where $p < 0.01$; * where $p < 0.05$; * where $p < 0.1$).

	1907–50	1907–83	1951–83	1907–2016
PREC annual	18.8	43.8***	94.4*	45.1***
Std. err.	4.144	1.583	5.316	1.426
p value	0.654	0.008	0.089	0.003
PREC SON	9.14	16.8***	30.3	15.7***
Std. err.	1.247	0.542	2.215	0.422
p value	0.468	0.002	0.183	0.0004
PREC DJF	12.3	13.0**	−7.80	10.3**
Std. err.	1.648	0.590	1.948	0.494
p value	0.459	0.031	0.692	0.041
PREC MAM	−9.11	10.9*	15.6	15.2***
Std. err.	1.460	0.621	2.497	0.487
p value	0.537	0.082	0.538	0.003
PREC JJA	17.8	9.60	48.3**	15.3**
Std. err.	2.119	0.745	1.824	0.611
p value	0.406	0.202	0.014	0.014

first, increasing precipitation appears to commence from the beginning of the twentieth century; and second, the increases appear to occur mainly over the autumn and winter months. The difference in temperature and precipitation trends (both the timing of the changes and the seasonality) suggests different climate drivers. Several other records from nearby meteorological stations also observe a long-term increase in precipitation, including the annual precipitation recorded on the Falklands Islands (Lister and Jones 2014; P. Jones et al. 2016) and greatly increased snow accumulation on the Antarctic Peninsula (Thomas et al. 2008). To elucidate the dominant atmospheric circulation that might explain the observed climate and weather extremes over South Georgia, we utilized 20CRv2c. (Compo et al. 2011) (Figs. 7, 8).

Mechanisms of change

We investigate the total precipitation in autumn and winter (March–August) and compare it to both 850-hPa geopotential height and 850-hPa meridional wind over the period 1905–83 (the data gap between 1983 and 2010 unfortunately prevents analysis in recent decades). From this analysis, we observed a correlation between low pressure over South America and precipitation at South Georgia, resulting from the delivery of moisture via northerly and easterly airflow over South Georgia (Fig. 7). Although the Amundsen Sea low is generally associated with quasi-stationary, low pressure systems to the west of the Antarctic Peninsula (Hosking et al. 2013), it has synoptic-scale influences, with large seasonal variability that can be manifested by low pressure systems developing farther north (Fogt et al. 2012). Our analysis shows these synoptic conditions are associated with higher precipitation over South Georgia. The increasing trends in rainfall from the South Georgia climate records are in general agreement with Turney et al. (2016c), who describe higher rainfall over the Falkland Islands from the 1940s (as reported in Lister and Jones 2014); this is consistent with a lower mean sea level pressure in the South Atlantic and higher pressure in the Amundsen Sea low, leading to an unprecedented increase in growth of peat sequences relative to the last 6000 years. Similar findings from the Antarctic Peninsula, with increased precipitation (Thomas et al. 2008) and temperature (Thomas et al. 2009) driving an increase in moss bank growth (Amesbury et al. 2017), also support our findings.

However, while the above mechanisms dominate in winter and can cause enhanced precipitation over South Georgia, there appears to have been a seasonal change in the configuration of the synoptic conditions,

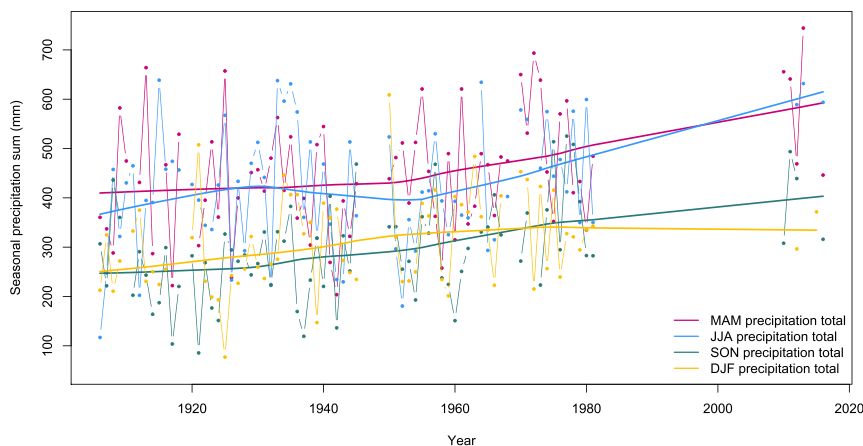


FIG. 6. Seasonal precipitation totals, including only years with <3 missing days per season, each with a locally weighted scatterplot smoothing (1905–2016).

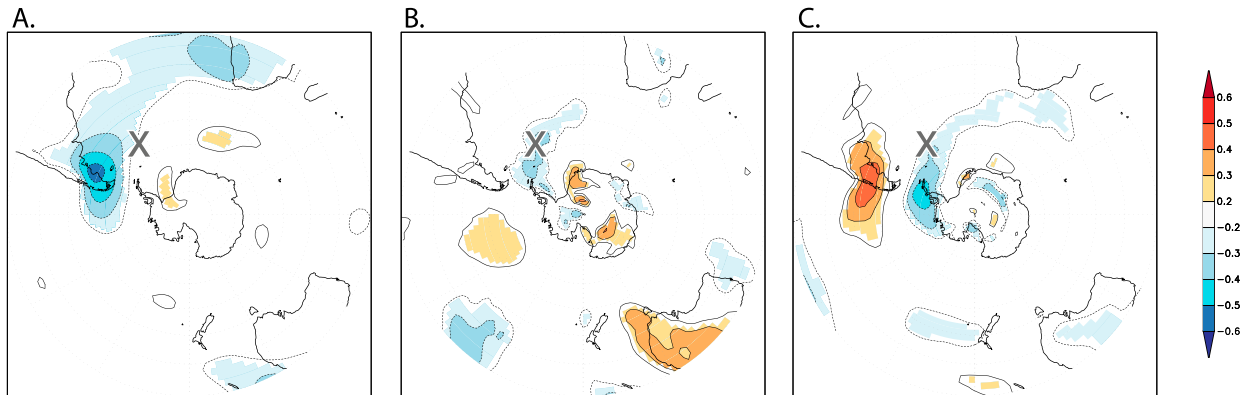


FIG. 7. Correlations between the detrended and deseasonalized monthly precipitation sum from South Georgia (marked with an “X”) and (a) 850-hPa geopotential height, (b) 850-hPa meridional wind, and (c) 850-hPa zonal wind, averaged over March–August over the period 1905–83 using 20CRv2c. Significance $p_{\text{field}} < 0.1$. Analyses were made with KNMI Climate Explorer (van Oldenborgh and Burgers 2005).

consistent with the summer impact of SAM. We therefore investigated the summer months (December–February) comparing mean monthly temperature with 850-hPa geopotential height and 850-hPa zonal wind to

understand the mechanisms of synoptic change. To compare trends over the twentieth century, we split our data into an “early” period (1905–50) and a “late” period (1950–2016). Our analysis finds a strengthening

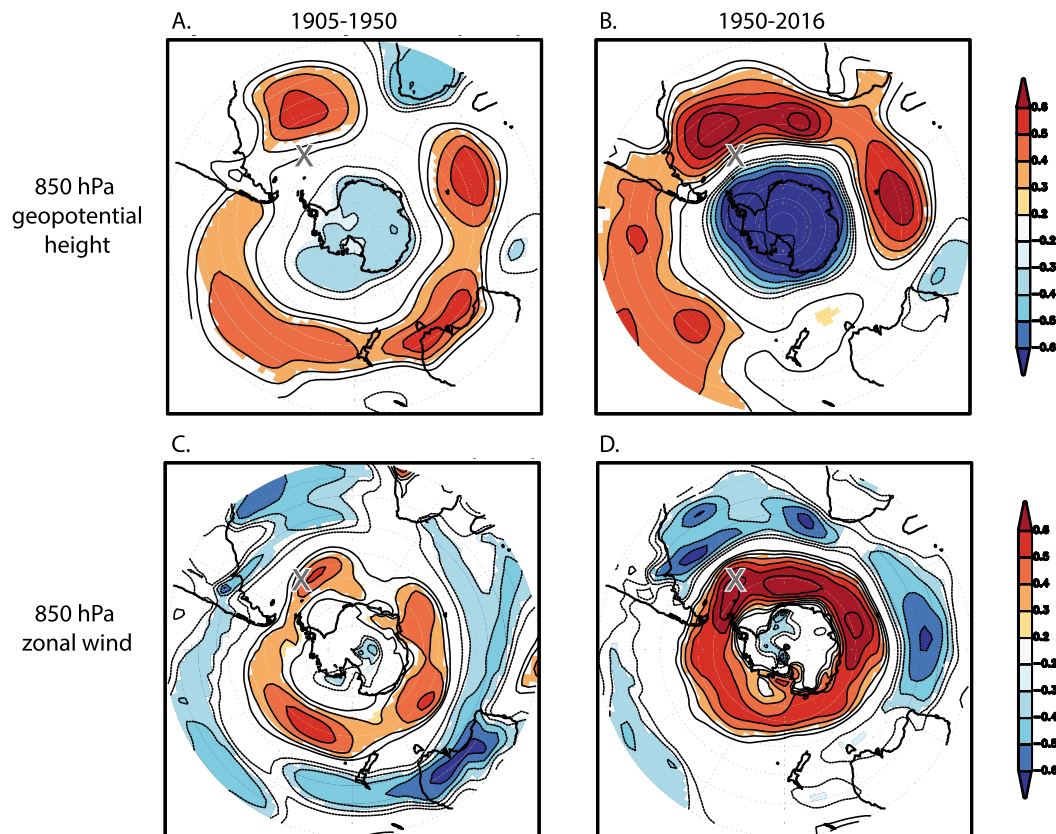


FIG. 8. Correlations between the detrended and deseasonalized mean monthly temperature from South Georgia (marked with an “X”) and (a) 850-hPa geopotential height (1905–50), (b) 850-hPa geopotential height (1951–2016), (c) 850-hPa zonal wind (1905–50), and (d) 850-hPa zonal wind (1951–2016), averaged over December–February using 20CRv2c. Significance $p_{\text{field}} < 0.1$. Analyses were made with KNMI Climate Explorer (van Oldenborgh and Burgers 2005).

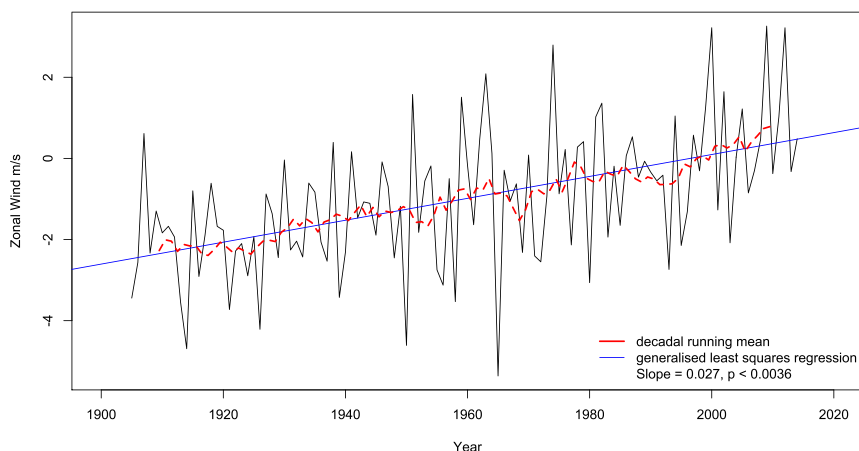


FIG. 9. Zonal wind speed at 850 hPa from 20CRv2c averaged over DJF at South Georgia, with generalized least squares regression (blue) and decadal running mean (red) lines shown.

correlation between temperature and high-latitude zonal airflow over the twentieth century, resulting from a poleward shift in the circumpolar trough during the summer (Fig. 8). Based on these results, we investigate the 20CRv2 time series of 850-hPa zonal wind over South Georgia, averaged over December–February, and detect a significant ($p < 0.036$) increasing trend in the zonal wind (Fig. 9). While further work is needed to increase the density of early observations in reanalysis products (such as the data reported in this paper), the inferred changing synoptic conditions are generally consistent with both independent climate observations and proxy data (Turney et al. 2016c; Amesbury et al. 2017; Thomas et al. 2008, 2009).

The above changes can give rise to surface warming over South Georgia. Although the link between increasing westerly winds and warming over South Georgia may at first seem counterintuitive, there is a demonstrated link between the strength of the westerly winds and the occurrence and magnitude of föhn winds (Bannister and King 2015). If the strength of the winds is sufficiently high, downslope winds develop on the (northeastern) leeside of the island, causing substantial temperature increases through the föhn wind mechanics, as discussed above. This link between föhn winds, westerly airflow, and higher temperatures helps to explain the slight offset in temperature between 20CRv2c (which is not sufficiently resolved to reconstruct föhn winds) and observations from South Georgia in recent decades. Regardless of the precise mechanism of the generation of the föhn winds, the relationship between the positive trend in SAM from the 1960s (Jones et al. 2009), enhancing westerly airflow over the island, and the increased frequency and magnitude of föhn winds, helps to explain the tendency for the high rate of

summer warming and increasing frequency of warm extremes that we observe in South Georgia over the past century.

5. Wider implications

Changes to the climatic and environmental conditions that shape the current biological diversity constitute the dominant threat to the island of South Georgia. Contemporary glacier retreat has resulted in the increased threat of invasive rat species from areas that were previously isolated due to ice barriers (Cook et al. 2010). However, while a recent program to eradicate rats was successfully implemented (Martin and Richardson 2017), further biological invasions and colonization of alien species are a continuing threat with the current and projected rates of regional climate change. The South Georgian shelf is the most speciose region of the Southern Ocean reported to date (Hogg et al. 2011), with a cumulative dominance of endemic and range-edge species, many of which, such as Antarctic krill *Euphausia superba*, show declining habitat suitability with warming temperatures (Whitehouse et al. 2008). This, in turn, has negative impacts on the breeding success of krill-dependent penguins and seals (Murphy et al. 2007). Improving our understanding of the impact of climate change is establishing link between synoptic-scale and mesoscale meteorological processes.

6. Conclusions

The data presented here underscore the importance of the rescue of historical, daily resolved data from subantarctic remote islands to disentangle seasonal and extreme changes. We find a significant average

temperature rise of $0.13^{\circ}\text{C decade}^{-1}$ over the period 1907–2016 ($p < 0.0001$), with most of this increase taking place during the latter half of the twentieth century, weighted toward the summer months. We also observe a long-term increase in precipitation over the same period ($45.1\text{ mm decade}^{-1}$, $p < 0.003$), with autumn and winter rainfall dominating this signal. Using atmospheric reanalysis, we demonstrate a link between increasing temperature trends and atmospheric circulation dominated by stronger westerly airflow, resulting in significant föhn-related warming, with potentially important implications for biodiversity and ecosystems in the region.

Acknowledgments. CT and ZT acknowledge the support of the Australian Research Council (FL100100195). This study is a contribution to the Atmospheric Circulation Reconstructions over the Earth (ACRE) initiative. RA is supported by funding from the Joint UK BEIS/Defra Met Office Hadley Centre Climate Programme (GA01101) and acknowledges the University of Southern Queensland, Toowoomba, Australia, where he is an adjunct professor. Support for the Twentieth Century Reanalysis project version 2c dataset is provided by the U.S. Department of Energy Office of Science—Biological and Environmental Research (BER) and by the National Oceanic and Atmospheric Administration Climate Program Office. We thank Gil Compo for valuable comments on the manuscript.

REFERENCES

- Abram, N. J., R. Mulvaney, F. Vimeux, S. J. Phipps, J. Turner, and M. H. England, 2014: Evolution of the southern annular mode during the past millennium. *Nat. Climate Change*, **4**, 564–569, <https://doi.org/10.1038/nclimate2235>.
- Alexander, L. V., and N. Herold, 2015: ClimPACTv2 indices and software. WMO, <https://github.com/ARCCSS-extremes/climpact2>.
- , and Coauthors, 2006: Global observed changes in daily climate extremes of temperature and precipitation. *J. Geophys. Res.*, **111**, D05109, <https://doi.org/10.1029/2005JD006290>.
- Amesbury, M. J., T. P. Roland, J. Royles, D. A. Hodgson, P. Convey, H. Griffiths, and D. J. Charman, 2017: Widespread biological response to rapid warming on the Antarctic Peninsula. *Curr. Biol.*, **27**, 1616–1622, <https://doi.org/10.1016/j.cub.2017.04.034>.
- Anderson, R., S. Ali, L. I. Bradtmiller, S. H. H. Nielsen, M. O. Fleisher, B. E. Anderson, and L. H. Burckle, 2009: Wind-driven upwelling in the Southern Ocean and the deglacial rise in atmospheric CO_2 . *Science*, **323**, 1443–1448, <https://doi.org/10.1126/science.1167441>.
- Bannister, D., and J. King, 2015: Föhn winds on South Georgia and their impact on regional climate. *Weather*, **70**, 324–329, <https://doi.org/10.1002/wea.2548>.
- Boyd, P. W., S. T. Lennartz, D. M. Glover, and S. C. Doney, 2015: Biological ramifications of climate-change-mediated oceanic multi-stressors. *Nat. Climate Change*, **5**, 71–79, <https://doi.org/10.1038/nclimate2441>.
- Compo, G. P., and Coauthors, 2011: The Twentieth Century Reanalysis project. *Quart. J. Roy. Meteor. Soc.*, **137**, 1–28, <https://doi.org/10.1002/qj.776>.
- Constable, A. J., and Coauthors, 2014: Climate change and Southern Ocean ecosystems I: How changes in physical habitats directly affect marine biota. *Global Change Biol.*, **20**, 3004–3025, <https://doi.org/10.1111/gcb.12623>.
- Cook, A. J., S. Poncet, A. P. R. Cooper, D. J. Herbert, and D. Christie, 2010: Glacier retreat on South Georgia and implications for the spread of rats. *Antarct. Sci.*, **22**, 255–263, <https://doi.org/10.1017/S0954102010000064>.
- Ding, Q., E. J. Steig, D. S. Battisti, and J. M. Wallace, 2012: Influence of the tropics on the southern annular mode. *J. Climate*, **25**, 6330–6348, <https://doi.org/10.1175/JCLI-D-11-00523.1>.
- Elvidge, A. D., and I. A. Renfrew, 2016: The causes of föhn warming in the lee of mountains. *Bull. Amer. Meteor. Soc.*, **97**, 455–466, <https://doi.org/10.1175/BAMS-D-14-00194.1>.
- Fogt, R. L., D. H. Bromwich, and K. M. Hines, 2011: Understanding the SAM influence on the South Pacific ENSO teleconnection. *Climate Dyn.*, **36**, 1555–1576, <https://doi.org/10.1007/s00382-010-0905-0>.
- , A. J. Wovrosh, R. A. Langen, and I. Simmonds, 2012: The characteristic variability and connection to the underlying synoptic activity of the Amundsen-Bellinghousen Seas Low. *J. Geophys. Res.*, **117**, D07111, <https://doi.org/10.1029/2011JD017337>.
- Førland, E. J., and I. Hanssen-Bauer, 2000: Increased precipitation in the Norwegian Arctic: True or false? *Climatic Change*, **46**, 485–509, <https://doi.org/10.1023/A:1005613304674>.
- , and —, 2001: Changes in temperature and precipitation in the Norwegian Arctic during the 20th century. *Detecting and Modeling Regional Climate Change*, M. B. India and D. L. Bonillo, Eds., Springer, 153–161, https://doi.org/10.1007/978-3-662-04313-4_14.
- Giese, B. S., H. F. Seidel, G. P. Compo, and P. D. Sardeshmukh, 2016: An ensemble of ocean reanalyses for 1815–2013 with sparse observational input. *J. Geophys. Res. Oceans*, **121**, 6891–6910, <https://doi.org/10.1002/2016JC012079>.
- Goodison, B. E., P. Y. T. Louie, and D. Yang, 1998: WMO solid precipitation measurement intercomparison. Instruments and Observing Methods Rep. 67, WMO/TD-872, 212 pp., <https://www.wmo.int/pages/prog/www/IMOP/publications/IOM-67-solid-precip/WMOtd872.pdf>.
- Gordon, J. E., V. M. Haynes, and A. Hubbard, 2008: Recent glacier changes and climate trends on South Georgia. *Global Planet. Change*, **60**, 72–84, <https://doi.org/10.1016/j.gloplacha.2006.07.037>.
- Hanssen-Bauer, I., 2002: Temperature and precipitation in Svalbard 1912–2050: Measurements and scenarios. *Polar Rec.*, **38**, 225–232, <https://doi.org/10.1017/S0032247400017757>.
- Hogg, O. T., D. K. A. Barnes, and H. J. Griffiths, 2011: Highly diverse, poorly studied and uniquely threatened by climate change: An assessment of marine biodiversity on South Georgia's continental shelf. *PLoS One*, **6**, e19795, <https://doi.org/10.1371/journal.pone.0019795>.
- Hosking, J. S., A. Orr, G. J. Marshall, J. Turner, and T. Phillips, 2013: The influence of the Amundsen–Bellinghousen Seas low on the climate of West Antarctica and its representation in coupled climate model simulations. *J. Climate*, **26**, 6633–6648, <https://doi.org/10.1175/JCLI-D-12-00813.1>.
- IPCC, 2012: *Managing the Risks of Extreme Events and Disasters to Advance Climate Change Adaptation*. C. B. Field et al., Eds.,

- Cambridge University Press, 582 pp., https://www.ipcc.ch/pdf/special-reports/srex/SREX_Full_Report.pdf.
- Jones, J. M., R. L. Fogt, M. Widmann, G. J. Marshall, P. D. Jones, and M. Visbeck, 2009: Historical SAM variability. Part I: Century-length seasonal reconstructions. *J. Climate*, **22**, 5319–5345, <https://doi.org/10.1175/2009JCLI2785.1>.
- , and Coauthors, 2016: Assessing recent trends in high-latitude Southern Hemisphere surface climate. *Nat. Climate Change*, **6**, 917–926, <https://doi.org/10.1038/nclimate3103>.
- Jones, P. D., C. Harpham, and D. Lister, 2016: Long-term trends in gale days and storminess for the Falkland Islands. *Int. J. Climatol.*, **36**, 1413–1427, <https://doi.org/10.1002/joc.4434>.
- Landschützer, P., and Coauthors, 2015: The reinvigoration of the Southern Ocean carbon sink. *Science*, **349**, 1221–1224, <https://doi.org/10.1126/science.aab2620>.
- Le Quéré, C., M. R. Raupach, J. G. Canadell, and G. Marland, 2009: Trends in the sources and sinks of carbon dioxide. *Nat. Geosci.*, **2**, 831–836, <https://doi.org/10.1038/ngeo689>.
- Lister, D. H., and P. D. Jones, 2014: Long-term temperature and precipitation records from the Falkland Islands. *Int. J. Climatol.*, **35**, 1224–1231, <https://doi.org/10.1002/joc.4049>.
- Marshall, G. J., 2003: Trends in the southern annular mode from observations and reanalyses. *J. Climate*, **16**, 4134–4143, [https://doi.org/10.1175/1520-0442\(2003\)016<4134:TITSAM>2.0.CO;2](https://doi.org/10.1175/1520-0442(2003)016<4134:TITSAM>2.0.CO;2).
- Martin, A. R., and M. G. Richardson, 2017: Rodent eradication scaled up: Clearing rats and mice from South Georgia. *Oryx*, <https://doi.org/10.1017/S003060531700028X>.
- Mo, K. C., and R. W. Higgins, 1998: The Pacific–South American modes and tropical convection during the Southern Hemisphere winter. *Mon. Wea. Rev.*, **126**, 1581–1596, [https://doi.org/10.1175/1520-0493\(1998\)126<1581:TPSAMA>2.0.CO;2](https://doi.org/10.1175/1520-0493(1998)126<1581:TPSAMA>2.0.CO;2).
- Murphy, E. J., and Coauthors, 2007: Climatically driven fluctuations in Southern Ocean ecosystems. *Proc. Roy. Soc. London*, **274B**, 3057–3067, <https://doi.org/10.1098/rspb.2007.1180>.
- Richard, Y., and Coauthors, 2013: Temperature changes in the mid- and high- latitudes of the Southern Hemisphere. *Int. J. Climatol.*, **33**, 1948–1963, <https://doi.org/10.1002/joc.3563>.
- Sallée, J.-B., R. J. Matear, S. R. Rintoul, and A. Lenton, 2012: Localized subduction of anthropogenic carbon dioxide in the Southern Hemisphere oceans. *Nat. Geosci.*, **5**, 579–584, <https://doi.org/10.1038/ngeo1523>.
- Sardeshmukh, P. D., G. P. Compo, and C. Penland, 2015: Need for caution in interpreting extreme weather statistics. *J. Climate*, **28**, 9166–9187, <https://doi.org/10.1175/JCLI-D-15-0020.1>.
- Skansi, M., and Coauthors, 2017: Evaluating highest temperature extremes in the Antarctic. *Eos, Trans. Amer. Geophys. Union*, **98**, <https://doi.org/10.1029/2017EO068325>.
- Thomas, E. R., G. J. Marshall, and J. R. McConnell, 2008: A doubling in snow accumulation in the western Antarctic Peninsula since 1850. *Geophys. Res. Lett.*, **35**, L01706, <https://doi.org/10.1029/2007GL032529>.
- , P. F. Dennis, T. J. Bracegirdle, and C. Franzke, 2009: Ice core evidence for significant 100-year regional warming on the Antarctic Peninsula. *Geophys. Res. Lett.*, **36**, L20704, <https://doi.org/10.1029/2009GL040104>.
- Thomas, Z. A., 2016: Using natural archives to detect climate and environmental tipping points in the Earth system. *Quat. Sci. Rev.*, **152**, 60–71, <https://doi.org/10.1016/j.quascirev.2016.09.026>.
- Thompson, D. W. J., and S. Solomon, 2002: Interpretation of recent Southern Hemisphere climate change. *Science*, **296**, 895–899, <https://doi.org/10.1126/science.1087440>.
- , —, P. J. Kushner, M. H. England, K. M. Grise, and D. J. Karoly, 2011: Signatures of the Antarctic ozone hole in Southern Hemisphere surface climate change. *Nat. Geosci.*, **4**, 741–749, <https://doi.org/10.1038/ngeo1296>.
- Trathan, P. N., J. Forcada, and E. J. Murphy, 2012: Environmental forcing and Southern Ocean marine predator populations: Effects of climate change and variability. *Antarctic Ecosystems: An Extreme Environment in a Changing World*, A. D. Rogers et al., Eds., John Wiley & Sons, 335–353.
- Turner, J., and Coauthors, 2005: Antarctic climate change during the last 50 years. *Int. J. Climatol.*, **25**, 279–294, <https://doi.org/10.1002/joc.1130>.
- Turney, C. S. M., and Coauthors, 2016a: Intensification of Southern Hemisphere westerly winds 2000–1000 years ago: Evidence from the subantarctic Campbell and Auckland Islands (52–50°S). *J. Quat. Sci.*, **31**, 12–19, <https://doi.org/10.1002/jqs.2828>.
- , and Coauthors, 2016b: Multidecadal variations in Southern Hemisphere atmospheric ¹⁴C: Evidence against a Southern Ocean sink at the end of the Little Ice Age CO₂ anomaly. *Global Biogeochem. Cycles*, **30**, 211–218, <https://doi.org/10.1002/2015GB005257>.
- , and Coauthors, 2016c: Anomalous mid-twentieth century atmospheric circulation change over the South Atlantic compared to the last 6000 years. *Environ. Res. Lett.*, **11**, 064009, <https://doi.org/10.1088/1748-9326/11/6/064009>.
- , and Coauthors, 2017: Tropical forcing of increased Southern Ocean climate variability revealed by a 140-year subantarctic temperature reconstruction. *Climate Past*, **13**, 231–248, <https://doi.org/10.5194/cp-13-231-2017>.
- van Oldenborgh, G. J., and G. Burgers, 2005: Searching for decadal variations in ENSO precipitation teleconnections. *Geophys. Res. Lett.*, **32**, L15701, <https://doi.org/10.1029/2005GL023110>.
- Visbeck, M., 2009: A station-based southern annular mode index from 1884 to 2005. *J. Climate*, **22**, 940–950, <https://doi.org/10.1175/2008JCLI2260.1>.
- Wang, X. L., 2008a: Accounting for autocorrelation in detecting mean shifts in climate data series using the penalized maximal *t* or *F* test. *J. Appl. Meteor. Climatol.*, **47**, 2423–2444, <https://doi.org/10.1175/2008JAMC1741.1>.
- , 2008b: Penalized maximal *F* test for detecting undocumented mean shift without trend change. *J. Atmos. Oceanic Technol.*, **25**, 368–384, <https://doi.org/10.1175/2007JTECHA982.1>.
- , and Y. Feng, 2013: RHtestsV4 user manual. ETCCDI Tech Rep., 29 pp., http://etccdi.pacificclimate.org/RHtest/RHtestsV4_UserManual_20July2013.pdf.
- Whitehouse, M. J., M. P. Meredith, P. Rothery, A. Atkinson, P. Ward, and R. E. Korb, 2008: Rapid warming of the ocean around South Georgia, Southern Ocean, during the 20th century: Forcings, characteristics and implications for lower trophic levels. *Deep Sea Res. I*, **55**, 1218–1228, <https://doi.org/10.1016/j.dsr.2008.06.002>.
- Zazulie, N., M. Rusticucci, and S. Solomon, 2010: Changes in climate at high southern latitudes: A unique daily record at Orcadas spanning 1903–2008. *J. Climate*, **23**, 189–196, <https://doi.org/10.1175/2009JCLI3074.1>.
- Zhang, X., L. Alexander, G. C. Hegerl, P. Jones, A. K. Tank, T. C. Peterson, B. Trewin, and F. W. Zwiers, 2011: Indices for monitoring changes in extremes based on daily temperature and precipitation data. *Wiley Interdiscip. Rev.: Climate Change*, **2**, 851–870, <https://doi.org/10.1002/wcc.147>.